



Dual-comb ranging with frequency combs from single cavity free-running laser oscillators

JACOB NÜRNBERG, BENJAMIN WILLENBERG,  CHRISTOPHER R. PHILLIPS, *  AND URSULA KELLER 

Department of Physics, Institute for Quantum Electronics, ETH Zürich, 8093 Zürich, Switzerland
*cphillips@phys.ethz.ch

Abstract: Laser ranging (LIDAR) with dual optical frequency combs enables high-resolution distance measurements over long ranges with fast update rates. However, the high complexity of stabilized dual optical frequency comb systems makes it challenging to use this technique in industrial applications. To address this issue, here we demonstrate laser ranging directly from the output of both a free-running dual-comb diode-pumped semiconductor and solid-state laser oscillator. Dual-comb operation from a single cavity is achieved via polarization duplexing with intracavity birefringent crystals. We perform ranging experiments with two implementations of this scheme: a modelocked integrated external cavity surface-emitting laser (MIXSEL) and a Yb:CaF₂ solid-state laser. For these proof of principle demonstrations, we measure the distance to a moving mirror mounted on a home-made shaker. The MIXSEL laser has a repetition rate of 2.736 GHz and a repetition rate difference of 52 kHz, and yields a measurement resolution of 1.36 μm. The Yb:CaF₂ laser has a repetition rate of 137 MHz and a repetition rate difference of 952 Hz, and yields a measurement resolution of 0.55 μm. In both cases the resolution is inferred by a parallel measurement with a HeNe interferometer. These results represent the first laser ranging with free-running dual-comb solid-state oscillators. With further optimization, resolution well below 1 μm and range well above 1 km are expected with this technique.

© 2021 Optical Society of America under the terms of the [OSA Open Access Publishing Agreement](#)

1. Introduction

Modern day technological advancements demand solutions to fast distance measurements with high precision and range. Any distance measurement is quantified by precision and accuracy, ambiguity range and by the update rate. Laser based ranging has proven to be fast and reliable even for more sophisticated ranging challenges in a wide variety of fields including object detection and recognition.

Interferometric laser ranging systems, such as a Michelson interferometer, determine the phase shift of a signal after traversing an unknown distance. Although they provide sub-wavelength resolution, these systems have an extremely short ambiguity range on the scale of the wavelength itself. Multiwavelength interferometers achieve increased but still limited ambiguity ranges through the generation of a synthetic longer wavelength [1–4].

The limited range of traditional interferometric techniques can be overcome by light detection and ranging (LIDAR), where the optical delay of a pulsed or modulated waveform is used to infer distance. The two dominant approaches, namely time of flight LIDAR and frequency-modulated continuous-wave LIDAR, have shown sub-millimeter precision over large ambiguity ranges [5–7]. Using frequency combs, various approaches have shown long ambiguity ranges with high precision and fast scanning speeds by leveraging simultaneous heterodyne or superheterodyne detection [6,8–10].

In LIDAR with dual optical frequency combs (dual-combs), ranging is achieved by exploiting the time scaling within the beatnote of two mutually coherent frequency combs in a similar manner to equivalent time sampling [11,12]. Dual-comb LIDAR has the advantage of simultaneously offering long range and high resolution without requiring any moving mechanical parts to scan

delay. The first demonstration in 2009 was based on two stabilized fiber frequency combs [13]. Since then, similar measurements have been demonstrated with free running fiber combs [14], including single-cavity fiber based systems [15–17], and microresonator based frequency combs [18,19].

Here, we present dual-comb LIDAR experiments using two types of free-running dual-comb laser oscillators: a modelocked integrated external cavity surface-emitting laser (MIXSEL) [20], and a solid-state laser. The lasers themselves were presented previously [21,22]; the MIXSEL was applied to dual-comb spectroscopy, while the solid-state laser was applied to pump-probe sampling. In both of these lasers, we use polarization duplexing with intracavity birefringent crystals to generate two frequency combs from a single laser cavity [23]. A small and adjustable repetition rate difference is obtained by inserting a pair of 45°-cut birefringent crystals into the cavity. We perform ranging experiments with the dual-comb MIXSEL and compare the results to the dual-comb Yb:CaF₂ laser. With the MIXSEL, we sample at an update rate of 52 kHz with a resolution of 1.36 μm. The Yb:CaF₂ laser achieves an even higher resolution of 0.55 μm but at a lower update rate of 952 Hz. These results represent, to the best of our knowledge, the first dual-comb ranging with free-running MIXSELS and diode-pumped solid-state lasers.

The use of such lasers is attractive for LIDAR due to their ultra-low intensity and timing noise properties, especially at high frequencies [24,25]. Moreover, they can achieve high average power, and operate over a wide range of repetition rates up to 100 GHz [26], meaning that their parameters can be tailored for optimal LIDAR sensitivity and range. The main drawback of the free-space cavity layouts typically used is their sensitivity to mechanical disturbances. However, by using a single-cavity dual-comb laser approach [23], we are able to overcome this drawback. Note that similar dual-comb laser concepts have been widely explored by several groups in recent years, as reviewed in [27]. The common path of the combs inside the cavity increases their mutual stability and therefore mitigates the need for active stabilization. Additionally, the resulting system is very simple since only one passively-stable laser oscillator is required. Therefore, our results pave the way for a new class of versatile dual-comb LIDAR systems for scientific and industrial applications.

2. Experimental setup

For dual-comb ranging, the first frequency comb, denoted as signal (S), samples the distance between a reference plane (R) and the target (T). The other comb takes the role of a local oscillator (LO). After recombination, the distance information is encoded in the interference of the two combs.

Figure 1(a) depicts the measurement setup used in the following experiments. The lasers generate two frequency combs with perpendicular polarization states. We separate signal (red) and local oscillator comb (blue) with a polarizing beam splitter cube (PBS). A half-wave plate rotates the polarization of the local oscillator to coincide with the signal comb. The signal comb passes through a partially reflective reference fused silica wedge and is directed with two mirrors towards the target. The target is a mirror mounted to a home built shaker oscillating with a frequency of 10 Hz. The reflections of the reference and the target are recombined with the local oscillator in a non-polarizing beam splitter cube. The signal is then recorded with a 5-GHz photodiode (Thorlabs DET08CL) and a digitizing oscilloscope (Teledyne LeCroy WAVEPRO 254HD, bandwidth 2.5 GHz). We use analog lowpass (LP) and bandpass (BP) filters as listed in Table 1 at the input of the oscilloscope to filter out the pulse repetition rates and reduce noise in unwanted frequency bands. Additionally, we monitor the pulse repetition rates of signal $f_{\text{rep},s}$ and local oscillator $f_{\text{rep},lo}$ with separate photodetectors on the same oscilloscope. To verify our ranging measurements, we integrate a Michelson type interferometer based on a helium-neon laser (HeNe, $\lambda = 632.8$ nm) with a dichroic mirror into the setup.

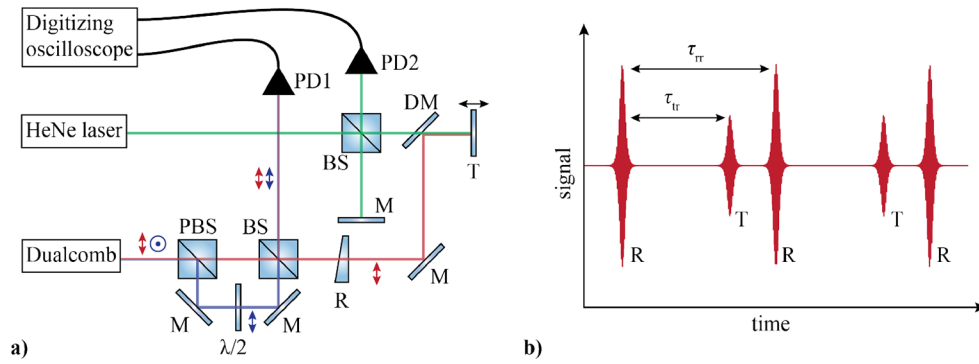


Fig. 1. (a) Schematic of the measurement setup. The signal frequency comb (red) samples the distance between the back facet of a reference wedge (R) and the target (T). An interferogram is recorded with a photodiode and an oscilloscope, after recombining signal and local oscillator (blue) in a beam splitter (BS). In addition a classical Michelson type interferometer (green beam path) is integrated in the setup to track the position changes of the target. (b) A typical interferogram. Interference occurs when the backreflections of the target (T) and reference (R) interfere with the local oscillator. The delay between target and reference interference τ_{tr} encodes the measured distance. The signal repeats every $\tau_{rr} = 1/\Delta f_{rep}$.

Table 1. Laser, measurement, and analysis parameters for ranging experiments with both lasers. The ambiguity range is given by the effective cavity length in air $L_{cav} = v_{g,air}/(2f_{rep,s})$ [13]. The values in the “Laser parameter” section of the table correspond to those of the lasers as published in [21,22]. Power per comb refers to the optical power in each of the orthogonally polarized combs at the output of the laser. Sampling rates and filter bandwidth were adapted according to the wavelengths of the respective laser. λ : center wavelength. $\Delta\lambda$: full-width at half-maximum (FWHM) bandwidth. τ_p : FWHM pulse duration

		MIXSEL	Yb:CaF ₂ laser
Laser parameters	λ	1028 nm	1050 nm
	$\Delta\lambda$	3 nm	6.9 nm
	τ_p	≈ 390 fs	≈ 175 fs
	power per comb	≈ 25 mW	≈ 440 mW
LIDAR parameters	f_{rep}	2.736 GHz	136.56 MHz
	Δf_{rep}	52.190 kHz	952 Hz
	ambiguity range	54.8 mm	1098.4 mm
Electronics	sampling rate	10 GS/s	1 GS/s
	recording time	50 ms	500 ms
	analog filters	bandpass 500-1000 MHz	lowpass 0-48 MHz
Analysis	digital filters	BP 580-625 MHz	None
	# of signals	2609	475

When both combs interfere, each back reflection causes an interferogram in the time domain as shown in Figure 1(b). Our data analysis follows previous publications [13,19]. The optical delay τ_{opt} between the two reflections is up-converted to electronically accessible time scales as

$$\tau_{tr} = \frac{1}{\alpha} \tau_{opt} = \frac{f_{rep,s}}{f_{rep,s} - f_{rep,lo}} \cdot \tau_{opt}. \quad (1)$$

Here, τ_{tr} is the measured delay between a target and a reference interferogram. Additionally, we measure the delay between two reference interferograms $\tau_{\text{rr}} = 1/\Delta f_{\text{rep}}$. The optical delay expressed in terms of electronically measurable quantities reads as

$$\tau_{\text{opt}} = \frac{\tau_{\text{tr}}}{\tau_{\text{rr}}} \cdot \frac{1}{f_{\text{rep},s}}. \quad (2)$$

The distance is then calculated by taking into account the group velocity of air, denoted $v_{g,\text{air}} = c/n_{g,\text{air}}$

$$d = \frac{1}{2} \left(v_{g,\text{air}} \tau_{\text{opt}} + \frac{M v_{g,\text{air}}}{f_{\text{rep},s}} \right) = \frac{1}{2} v_{g,\text{air}} \tau_{\text{opt}} + M L_{\text{cav}} \quad (3)$$

with an integer M . The second term accounts for the ambiguity of the signal for subsequent pulses. The pulses repeat every $T_{\text{rep},s} = 1/f_{\text{rep},s} = 2 \sum_i L_i / v_{g,i}$ where the sum iterates over all cavity elements. The ambiguity range is then set by the effective cavity length in air $L_{\text{cav}} = v_{g,\text{air}} / (2f_{\text{rep},s})$.

As the signal repeats for each multiple of the cavity length, the measured distance $\delta = d - M L_{\text{cav}}$ is mapped to the interval $[0, L_{\text{cav}}]$. The update rate corresponds to the difference in pulse repetition rate of the two lasers Δf_{rep} and is equivalent to the inverse of the delay between two subsequent reference signals $\tau_{\text{rr}} = 1/\Delta f_{\text{rep}} = (f_{\text{rep},s} - f_{\text{rep},lo})^{-1}$.

When measuring optical paths containing group delay dispersion, the sample pulses could become stretched, potentially reducing the resolution. However, the phase information from group delay dispersion is also encoded in the sample pulses, and this information could be used to find the peaks with the same accuracy as in a dispersion-free optical path.

For distance measurements, we use the dual-comb MIXSEL presented in [21] and the Yb:CaF₂ solid-state laser described in [22]. The semiconductor laser operates at a wavelength of 1028 nm and generates 25 mW average power per comb. The pulse repetition rate of 2.73 GHz sets the ambiguity range of this system to 54.8 mm and the difference in pulse repetition is 52 kHz.

The Yb:CaF₂ laser operates at 1050 nm. It has a lower pulse repetition rate of 136.56 MHz, corresponding to an ambiguity range of 1098.4 mm. If the repetition rate difference is set too high, then aliasing can occur on the down-converted RF signal. To avoid this, with a large safety margin, the difference in pulse repetition rate was set to 952 Hz. The laser can achieve between 250 mW and 440 mW of average power per comb. For ranging, we operate the laser at 270 mW per comb, which easily exceeds the power limitations of our photodetectors. To prevent saturation, we use the reflection of a fused silica wedge for the measurements.

To facilitate stable and reliable modelocking, we stabilize the heatsink temperature for the gain medium (semiconductor chip or gain crystal) in both lasers. An additional stabilization on the frequency combs or their relative parameters Δf_{rep} and Δf_{CEO} is not employed during the experiments. The mutual stability due to the common cavity satisfies the requirements for our experiments.

Due to the different gain configuration, the two lasers have different central wavelength, bandwidth, and pulse duration. To remove unwanted chromatic effects, we exchange all optics within the setup before using the other laser. Furthermore, the pulse repetition rates affect the necessary sampling rates and filter bandwidths. Table 1 lists the key laser and measurement parameters for both systems.

3. Dual-comb MIXSEL ranging

Figure 2(a) shows the recorded time domain signal for ranging experiments with the free-running dual-comb MIXSEL. The LO comb scans the signal comb every $\Delta T_{\text{rep}} = 1/\Delta f_{\text{rep}} \approx 19 \mu\text{s}$, before the signal repeats. Per full scan, we observe interference peaks of reference (R) and target (T) as well as additional stray reflections. Stray reflections, as indicated in Figure 2(a), however are easily identified by their amplitude and do not affect the measurement. The down-converted

signal of the dual-comb MIXSEL resides around 600 MHz. To suppress noise outside of this frequency range, we employ a 500 MHz to 1000 MHz analog BP filter for this measurement (Table 1).

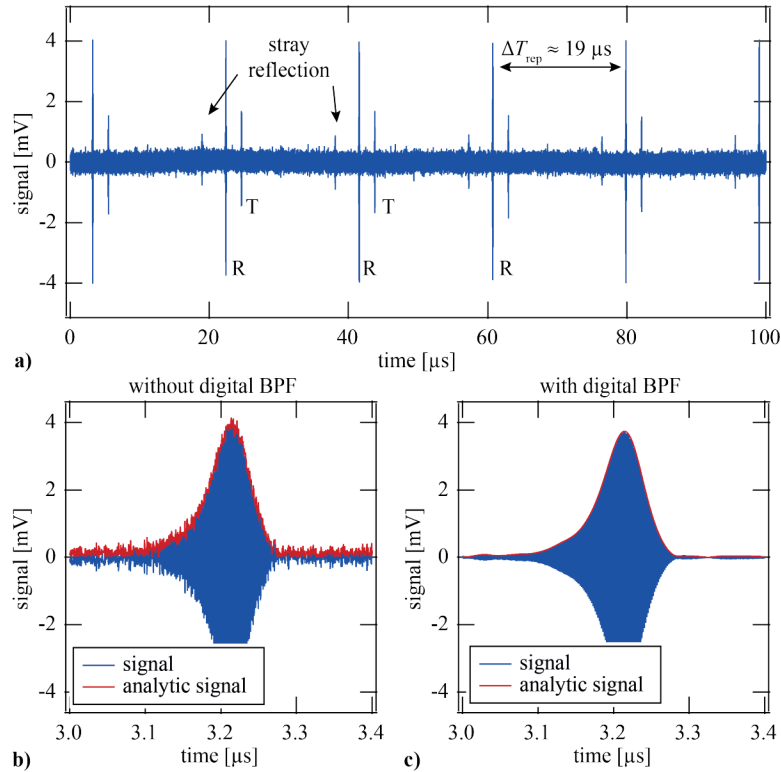


Fig. 2. (a) The recorded signal with the free-running dual-comb MIXSEL repeats every $\Delta T_{\text{rep}} = 19 \mu\text{s}$. Stray reflections are identified by their amplitude and do not distort the evaluation in a narrow time window around reference (R) and target (T) interferogram. (b) The time windowed interferogram (blue) and the absolute value of its analytic signal (red) are subject to a significant amount of noise. (c) With a narrow digital bandpass filter around the multiheterodyne radio frequency beat note of the optical frequency combs, the noise is reduced and the position in time can reliably be determined.

To infer the distance from the measured data, we extract the analytic signal for each interferogram through a Hilbert transform to determine its position in time. However, interferogram and analytic signal are still subject to a significant amount of noise (Figure 2(b)). To avoid distortions when determining the interferogram maximum position, we add an additional digital bandpass filter in the range from 580 MHz to 625 MHz. Therefore, in the frequency domain, we multiply the signal with a double sided hyperbolic tangent with an edge width of 10 MHz. After this treatment, noise on the analytic signal is heavily reduced (Figure 2(c)).

To determine the delay between signal pulses reflected from the reference versus pulses reflected from the target we extract the temporal position of the peaks in the interferogram trace with a two-step approach: First we perform an approximate peak search on the analytic signal. Next, the precise time is found by calculating the first-order moment of the magnitude squared of the analytic signal in a narrow time window of twice the full width at half maximum around the approximate peak times. A quadratically scaling first order moment $t_0 = \sum_i t_i |y_i|^2 / \sum_i |y_i|^2$, where $y(t)$ is the spectrally-filtered analytic signal, reliably yields the interferogram times and is robust

against systematic errors. Finally, we determine the measured distance from the delay between interferograms using Eqs. (2) and (3). Within a measurement time of 50 ms, we record 2609 full measurement periods, that we can evaluate for distance measurements. Memory limitations on our oscilloscope currently limit longer recordings for more than half a period of the shaker at 10 GS/s. The Michelson interferometer integrated into the setup yields a relative reference to confirm the validity of our measurement. We apply a standard phase fitting algorithm and fit an additional offset to match the LIDAR measurement and the Michelson data.

The results are shown in Figure 3(a) and show that we can reliably trace the 10 Hz shaker motion. It should be noted that this measurement was conducted around an absolute distance of 281 mm, or five times the ambiguity range of the laser. The measured distance is accordingly folded into the ambiguity range. Figure 3(b) displays the residuals between our LIDAR measurement and the Michelson reference with an rms deviation of 1.36 μm .

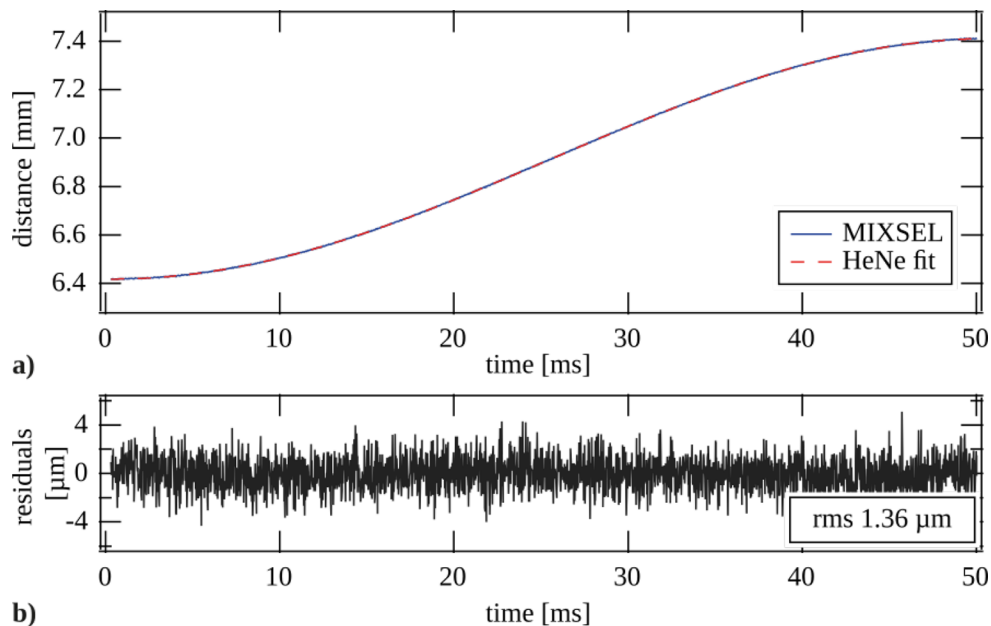


Fig. 3. (a) The distance measured with the dual-comb MIXSEL around 281 mm (solid blue) is folded into the ambiguity range and traces the 10 Hz motion of the shaker. It coincides with the reference recording from the Michelson interferometer (dashed red). (b) The residuals between dual-comb ranging and Michelson interferometer reveal an rms deviation of 1.36 μm .

4. Dual-comb solid state laser ranging

After exchanging all optics to match the emission wavelength of Yb:CaF₂, we perform an equivalent set of experiments with the free-running dual-comb Yb:CaF₂ laser. With the lower pulse repetition rate of this laser, we reduce the sampling rate and can record longer traces. The analog BP filters are replaced by LP filters with a 3 dB cutoff frequency at 48 MHz to suppress the pulse repetition rates in the radio frequency signal. Figure 4(a) shows the time domain recording with the signal repeating approximately every $1/\Delta f_{\text{rep}} \approx 1$ ms. The significantly higher signal-to-noise-ratio of the solid-state laser data is due to the higher power available in the setup when compared to the MIXSEL. The inset displays an individual interferogram as well as the magnitude of its analytic signal. The delay increment between subsequent pairs of pulses,

given approximately by $\Delta f_{\text{rep}}/f_{\text{rep}}^2$, is larger in the dual-comb solid-state laser, and the pulses are shorter. Consequently, the dual-comb interferogram consists of fewer oscillations. Additionally, interferogram and envelope show lower noise compared to the MIXSEL, such that an additional digital BP filter can be omitted in data analysis.

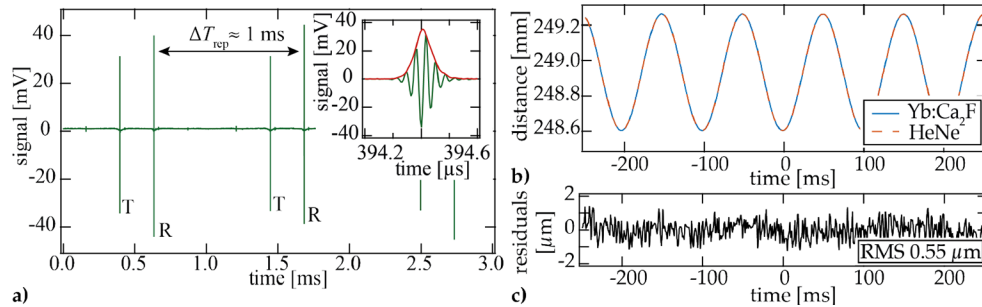


Fig. 4. (a) Target (T) and reference (R) interferograms recorded with the free-running dual-comb Yb:CaF₂ laser repeat every $\Delta T_{\text{rep}} \approx 1$ ms. The shorter pulses of the solid-state laser result in shorter interferograms with fewer cycles (inset, green). Less noise on the analytic signal (inset, red) avoids the need for additional digital filters. (b) The dual-comb Yb:CaF₂ laser (solid blue) reliably traces the absolute distance to the shaker of 248 mm within its ambiguity range. The measurement coincides with the reference from the Michelson interferometer (dashed red). The residuals amount to an rms deviation of 0.55 μm. (c) Difference between the two traces in (b).

The approach to data analysis is identical to the MIXSEL. The lower update rate of 952 Hz yields only 475 full signal periods over the experiment time of 500 ms. Figure 4(b) compares the retrieved distance measurements to the Michelson interferometer reference with the residuals shown in Figure 4(c). As with the MIXSEL, the data reveals the 10 Hz shaker motion. With the longer cavity length of the solid-state laser, this measurement yields the absolute distance around 249 mm within the first ambiguity range of the system. The residuals over the measurement period amount to an rms deviation of 0.55 μm.

5. Conclusion

In our experiments, we have shown that reliable and precise time-of-flight distance measurements within the ambiguity range are possible with free-running dual-comb semiconductor and solid-state laser systems. With the dual-comb MIXSEL the ambiguity range is 54.8 mm, and within one ambiguity range we demonstrate distance measurements with sub-2-μm precision at an update rate of above 50 kHz. Higher update rates could be achieved with a higher difference in pulse repetition rate, that can reach megahertz for the dual-comb MIXSEL as demonstrated in [23,28].

The dual-comb Yb:CaF₂ solid-state laser achieves ranging with a precision well below 1 μm and has an ambiguity range of 1098.4 mm. The repetition rate difference Δf_{rep} of the Yb:CaF₂ laser is set to 952 Hz. For faster measurements, these values could be increased somewhat before the onset of aliasing. With spectral filtering or scaling the pulse repetition rate of the lasers, it would be possible to increase Δf_{rep} significantly and achieve much higher update rates.

To increase the ambiguity range of the systems to exceed the cavity length, one can exploit the Vernier effect by interchanging the roles of the two frequency combs [13]. The theoretical extended ambiguity range under these conditions would be $R_A = v_{g,\text{air}}/2\Delta f_{\text{rep}} = 2.8$ km for the MIXSEL and 157 km for the solid-state laser. Under these conditions, both lasers are attractive for ground and drone based ranging solutions. In particular the higher update rate of the MIXSEL, when combined with the full extended ambiguity range, could make it highly suitable for applications requiring fast, long-range measurements.

Funding. Schweizerischer Nationalfonds zur Förderung der Wissenschaftlichen Forschung (40B2-0_180933).

Disclosures. The authors declare no conflicts of interest.

Data availability. Data underlying the results presented in this paper are not publicly available at this time but may be obtained from the authors upon reasonable request.

References

1. R. Dändliker, R. Thalmann, and D. Prongué, "Two-wavelength laser interferometry using superheterodyne detection," *Opt. Lett.* **13**(5), 339–341 (1988).
2. C. C. Williams and H. K. Wickramasinghe, "Absolute optical ranging with 200-nm resolution," *Opt. Lett.* **14**(11), 542–544 (1989).
3. J. A. Stone, A. Stejskal, and L. Howard, "Absolute interferometry with a 670-nm external cavity diode laser," *Appl. Opt.* **38**(28), 5981–5994 (1999).
4. H.-J. Yang, J. Deibel, S. Nyberg, and K. Riles, "High-precision absolute distance and vibration measurement with frequency scanned interferometry," *Appl. Opt.* **44**(19), 3937–3944 (2005).
5. S. M. Beck, J. R. Buck, W. F. Buell, R. P. Dickinson, D. A. Kozlowski, N. J. Marechal, and T. J. Wright, "Synthetic-aperture imaging laser radar: laboratory demonstration and signal processing," *Appl. Opt.* **44**(35), 7621–7629 (2005).
6. K. Minoshima and H. Matsumoto, "High-accuracy measurement of 240-m distance in an optical tunnel by use of a compact femtosecond laser," *Appl. Opt.* **39**(30), 5512–5517 (2000).
7. N. Bobroff, "Recent advances in displacement measuring interferometry," *Meas. Sci. Technol.* **4**(9), 907–926 (1993).
8. R. Fox and L. Hollberg, "Wavelength references for optical interferometry," in *CLEO/Europe. 2005 Conf. Lasers Electro-Optics Eur. 2005.*, vol. 44 (IEEE, 2005), p. 456.
9. N. Schuhler, Y. Salvadé, S. Lévêque, R. Dändliker, and R. Holzwarth, "Frequency-comb-referenced two-wavelength source for absolute distance measurement," *Opt. Lett.* **31**(21), 3101–3103 (2006).
10. Y. Salvadé, N. Schuhler, S. Lévêque, and S. Le Floch, "High-accuracy absolute distance measurement using frequency comb referenced multiwavelength source," *Appl. Opt.* **47**(14), 2715–2720 (2008).
11. P. A. Elzinga, F. E. Lytle, Y. Jian, G. B. King, and N. M. Laurendeau, "Pump/Probe Spectroscopy by Asynchronous Optical Sampling," *Appl. Spectrosc.* **41**(1), 2–4 (1987).
12. K. J. Weingarten, M. J. W. Rodwel, and D. M. Bloom, "Picosecond optical sampling of GaAs integrated circuits," *IEEE J. Quantum Electron.* **24**(2), 198–220 (1988).
13. I. Coddington, W. C. Swann, L. Nenadovic, and N. R. Newbury, "Rapid and precise absolute distance measurements at long range," *Nat. Photonics* **3**(6), 351–356 (2009).
14. T.-A. Liu, N. R. Newbury, and I. Coddington, "Sub-micron absolute distance measurements in sub-millisecond times with dual free-running femtosecond Er fiber-lasers," *Opt. Express* **19**(19), 18501–18509 (2011).
15. B. Lin, X. Zhao, M. He, Y. Pan, J. Chen, S. Cao, Y. Lin, Q. Wang, Z. Zheng, and Z. Fang, "Dual-comb absolute distance measurement based on a dual-wavelength passively mode-locked laser," *IEEE Photonics J.* **9**(6), 1–8 (2017).
16. D. Hu, Z. Wu, H. Cao, Y. Shi, R. Li, H. Tian, Y. Song, and M. Hu, "Dual-comb absolute distance measurement of non-cooperative targets with a single free-running mode-locked fiber laser," *Opt. Commun.* **482**, 126566 (2021).
17. J. Fellingner, G. Winkler, P. Aldia, A. S. Mayer, V. Shumakova, L. W. Perner, V. F. Pecile, T. Martynkien, P. Mergo, G. Sobo, and O. H. Heckl, "Simple approach for extending the ambiguity-free-range of dual-comb ranging," arXiv preprint arXiv:2106.05394 (2021).
18. M. G. Suh and K. J. Vahala, "Soliton microcomb range measurement," *Science* **359**(6378), 884–887 (2018).
19. P. Trocha, M. Karpov, D. Ganin, M. H. P. Pfeiffer, A. Kordts, S. Wolf, J. Krockenberger, P. Marin-Palomo, C. Weimann, S. Randel, W. Freude, T. J. Kippenberg, and C. Koos, "Ultrafast optical ranging using microresonator soliton frequency combs," *Science* **359**(6378), 887–891 (2018).
20. D. J. Maas, A. R. Bellancourt, B. Rudin, M. Golling, H. J. Unold, T. Südmeyer, and U. Keller, "Vertical integration of ultrafast semiconductor lasers," *Appl. Phys. B* **88**(4), 493–497 (2007).
21. J. Nürnberg, C. G. E. Alfieri, Z. Chen, D. Waldburger, N. Picqué, and U. Keller, "An unstabilized femtosecond semiconductor laser for dual-comb spectroscopy of acetylene," *Opt. Express* **27**(3), 3190–3199 (2019).
22. B. Willenberg, J. Pupekis, L. M. Krüger, F. Koch, C. R. Phillips, and U. Keller, "Femtosecond dual-comb Yb:CaF₂ laser from a single free-running polarization-multiplexed cavity for optical sampling applications," *Opt. Express* **28**(20), 30275–30288 (2020).
23. S. M. Link, A. Klenner, M. Mangold, C. A. Zaugg, M. Golling, B. W. Tilma, and U. Keller, "Dual-comb modelocked laser," *Opt. Express* **23**(5), 5521–5531 (2015).
24. S. Schilt, N. Bucalovic, V. Dolgovskiy, C. Schori, M. C. Stumpf, G. D. Domenico, S. Pekarek, A. E. H. Oehler, T. Südmeyer, U. Keller, and P. Thomann, "Fully stabilized optical frequency comb with sub-radian ceo phase noise from a sesam-modelocked 1.5- μ m solid-state laser," *Opt. Express* **19**(24), 24171–24181 (2011).
25. T. D. Shoji, W. Xie, K. L. Silverman, A. Feldman, T. Harvey, R. P. Mirin, and T. R. Schibli, "Ultra-low-noise monolithic mode-locked solid-state laser," *Optica* **3**(9), 995–998 (2016).
26. M. Mangold, C. A. Zaugg, S. M. Link, M. Golling, B. W. Tilma, and U. Keller, "Pulse repetition rate scaling from 5 to 100 GHz with a high-power semiconductor disk laser," *Opt. Express* **22**(5), 6099–6107 (2014).

27. R. Liao, H. Tian, W. Liu, R. Li, Y. Song, and M. Hu, "Dual-comb generation from a single laser source: principles and spectroscopic applications towards mid-ir—a review," *JPhys Photonics* **2**(4), 042006 (2020).
28. S. M. Link, D. J. H. C. Maas, D. Waldburger, and U. Keller, "Dual-comb spectroscopy of water vapor with a free-running semiconductor disk laser," *Science* **356**(6343), 1164–1168 (2017).